ePDH online.com

Credit: 2 PDH

Course Title:

Mobility Control for Enhanced Oil Recovery Using Polymer Gels and Foams

Approved for Credit in All 50 States
Visit epdhonline.com for state specific information including Ohio's required timing feature.

3 Easy Steps to Complete the Course:

1. Read the Course PDF
2. Purchase the Course Online & Take the Final Exam
3. Print Your Certificate

New Insight from Visualization of Mobility Control for Enhanced Oil Recovery Using Polymer Gels and Foams

Bergit Brattekås and Martin A. Fernø

Abstract

Several enhanced oil recovery (EOR) methods have been designed and developed in the past decades to maintain economic production from mature reservoirs with declining production rates. This chapter discuss mitigation of poor sweep efficiency in layered or naturally fractured reservoirs. EOR methods designed for such reservoirs all aim to reduce flow through highly conductive pathways and delay early breakthrough in production wells. Two approaches within this EOR class, injection of foam and polymer, specifically aim to improve the mobility ratio between the injected EOR fluid and the reservoir crude oil. Reduction in fracture conductivity may be achieved by adding a crosslinking agent to a polymer solution to create polymer gel. This may also be combined with water or chemical chasefloods (e.g. foam) for integrated enhanced oil recovery (iEOR). Polymer gel and foam mobility control for use in fractured reservoirs are discussed in this chapter, and new knowledge from experimental work is presented. The experiments emphasized visualization and in situ imaging techniques: CT, MRI and PET. New insight to dynamic behaviour and local variations in fluid saturations during injections was achieved through the use of complementary visualization techniques.

Keywords: polymer gel, foam, fractured reservoirs, iEOR, *in situ* imaging

1. Introduction

Polymer gel as a conformance control technique is frequently applied in fractured reservoirs to reduce fracture conductivity close to production wells, but may also be applied to enhance oil recovery when used in the injection well to divert subsequent fluids injected from the fracture network into unswept matrix blocks. Fluid injection following a gel injection is here referred to as a *chaseflood*, and constitutes a range of EOR fluids depending on the reservoir

and availability. Waterflooding was used as the standard chaseflood in this work, and the reader may assume that water is injected if not otherwise specified.

Generally, polymer gels are mixed in fresh water before injection to the field to achieve long-term stability of the solution. In this work, polymer gels are made from saline brines and offer a significant advantage compared with fresh water gels because less interaction is expected between the gel and reservoir fluids when the gel solvent (most commonly water) is comparable to the formation brine, and gel blocking performance is significantly improved when combined with low-salinity waterfloods in *integrated EOR*—iEOR, a term used here to describe the process where two or more proven EOR techniques are combined or performed in a smart sequence. In heterogeneous and fractured reservoirs, the iEOR approach is particularly effective when polymer gels are combined with mobility control techniques such as foam. The conformance control offered by polymer gels reduces flow in the largest fractures, whereas foam reduces gas mobility and increases the volumetric sweep efficiency of the reservoir resulting in incremental oil recovery. Gas mobility is reduced when bubbles are formed to make the gas phase discontinuous and separated by thin liquid films called lamellae. Foam application is particularly suited for heterogeneous reservoirs and is a field scale proven technique for EOR at both immiscible and miscible conditions and for aquifer remediation.

To successfully apply polymer gels or foams their behaviour and flow properties in porous media must be accurately predicted on a variety of scales. New insight to dynamic behaviour and local variations in fluid saturations during injections may be achieved through the use of complementary visualization techniques. Three imaging techniques are reviewed in this chapter: X-ray computed tomography (CT), magnetic resonance imaging (MRI) and positron emission tomography (PET). The imaging techniques are used separately or combined to closely monitor flow processes and improve the understanding of EOR techniques and their underlying principles on core plug scale, and new results are discussed in this chapter.

2. Polymer gel placement in fractured systems

From a reservoir engineering point of view, achieving high sweep efficiency in the reservoir to maximize oil recovery represents a challenge when fractures are present. The fractures generally have permeabilities that exceed the rock matrix by several orders of magnitude and therefore represent thief zones for the injected EOR fluid. Rather than displacing oil from the oil-saturated rock matrix, the injected fluids channel through the fracture network towards the producer, resulting in low sweep efficiency and excess production of water or injected chemicals.

2.1. Gel or gelant injection

Polymer gel is usually injected to the field as a *gelant* solution—a mixture containing all chemical components, but not yet crosslinked to form a rigid and highly viscous polymer gel. Gelant in many ways resembles the standard polymer solution, but transforms into a gel depending on temperature conditions and time—the time it takes for a gelant to transform

into a rigid gel at a given temperature is known as the *gelation time*. Gelant may flow both in the porous matrix and the fractures as a result of the lower viscosity and smaller particles relative to gel. When formed, long polymer chains in the gel structure prevent the gel from flowing through the small pores of the porous media, thus gel is contained to fractures during injection. In field applications, gelant is generally pumped from the surface and enters the reservoir either as a gelant or as a weak gel, depending on reservoir temperature and pumping time. The placement process must be carefully designed because the two fluids deposit differently in the fracture volume, which influences the ability of the gel to reduce fracture conductivity and impact its performance during conformance control operations. Gel blocking capacity as a function of gel state (gelant or gel) has therefore been thoroughly investigated at core plug scale [1–7].

2.2. The leakoff process

Although formed gel cannot flow through porous media due to its structure, the gel solvent (a range of solvents may be used, here we discuss water only) may leave the gel and progress through the pore network if the viscous forces become high enough. This fluid transport, called *leakoff*, increases the concentration of the gel in the fracture, resulting in a more rigid gel structure with a higher resistance to pressure during chasefloods. When the gel loses water due to leakoff its mobility decreases compared to the continuously injected ("fresh") gel; fresh gel propagates through internal conduits within the concentrated gel called *wormholes* [3, 8–10]. The transport of water from the gel depends mainly on gel strength and differential pressures across the gel slug, in addition to rock wettability and two-phase flow functions, therein capillary forces. Reduction of flow in fractures or high permeability zones after placement of polymer gels have been reported [2, 10–15].

2.3. Gel mechanical strength-dependency on gel state during placement

The mechanical strength of a gel in a fracture is an indication of its blocking ability and is often determined in the laboratory by measuring the gel *rupture pressure*—the pressure at which the gel in the fracture breaks apart and permits fluids to pass through it. If the injection pressure exceeds, the rupture pressure of the gel during a chaseflood, the gel-filled fracture will be partially re-opened to flow and fluid channelling through the blocked fracture will start again [4, 5, 7, 16]. Measurements of rupture pressures in open fractures with defined geometries have shown that gel mechanical strength after placement is dependent on the gel state during placement [7]. Rupture pressures measured after formed gel placement with leakoff were often to be consistent and predictable. It is assumed that water mobilizes gel from the wormholes during chasefloods and is thereafter contained in the narrow flow channels constituting the wormholes. Because of this, efficient gel blocking may also be achieved after gel rupture and significant water throughput. Rupture pressures measured after gelant injection and subsequent *in situ* gel formation, a process referred to as *gelation*, were comparable to measurements during gel injection, but with more inconsistency. It was suggested that gelation did not always occur [7], because gelant may experience compositional changes that interfere with gelation upon contact with the reservoir rock and fluids [5, 17], e.g. cross-linker diffusion into the

surrounding matrix that may lead to gelation failure [16]. Although initially comparable, the blocking capacity over time during chasefloods was consistently higher for pre-formed gels compared with gels with *in situ* gelation. This was explained by the presence of wormholes that collapsed and re-opened depending on the injection pressure.

2.4. Gel volume alterations

The blocking capacity of a gel placed in a fracture is also determined by the ability of the gel to maintain its volume relative to the fracture volume. After placement, the gel may undergo processes that change its volume and impact the success of a chaseflood. Several processes, such as *syneresis* [18, 19], *dehydration* [20–23] and *gel swelling* [24, 25], have been studied experimentally using bulk gel, core plugs and micromodels. During syneresis and dehydration, the gel volume is reduced due to loss of water caused by chemical reactions over time, changes in pressure gradients or matrix capillary forces adjacent to the gel network. Other conditions, such as temperature, solvent composition, ionic strength and external electric field, are the main causes of gel swelling, which impact the gel volume without the loss of water by influencing the osmotic pressure balance between the gel network and its surroundings [26]. The behaviour of a polymer gel during EOR chasefloods will, in summary, depend on both the properties of the gel itself and on the external conditions in the reservoir.

3. Foam flooding of fractured systems

EOR techniques in fractured reservoirs rely on maximizing the contact area between the injected EOR fluid and the rock surface, and therefore, the EOR fluid must transport effectively within the fracture network [27]. Most fracture networks, however, are heterogeneous themselves, with varying fracture aperture, orientation and connectivity.

3.1. Gas mobility reduction

Heterogeneous fracture networks may result in poor sweep of the injected EOR fluid, and mobility control should be implemented to maximize contact. Two-phase flow within rough-walled fractures has previously been investigated using Newtonian fluids [28–30] and non-Newtonian polymer solutions [31, 32]. Foam has the potential to increase oil recovery by better areal sweep, better vertical sweep (less gravity override), less viscous fingering and diversion of gas from higher permeable or previously swept layers [33]. Diversion of gas into lower permeable layers using foams may be important for fractured systems, where a very large permeability contrast exists and cross-flow between the zones occur [34].

3.2. Foam generation in fractures

Foam is generated in porous media by snap-off, lamella division or leave-behind mechanisms. Foam generation is affected by porous medium topological properties, wetting content, capillary suction pressure, surfactant formulation, gas fractional flow and flow rate. Snap-off

and lamella division create "strong" foam in terms of separate gas bubbles above a critical capillary number [35], whereas leave-behind forms lamellae oriented parallel to the flow direction with only moderate effect on flow resistance, and the injected gas remains as a continuous phase. In porous media with permeability discontinuities, snap-off is an important mechanism for foam generation [36–38]. Foam generation within a fracture network was observed in a replica of a rough-walled fracture with variable aperture [39]. Foam was found to be generated by snap-off and the bubble size was four times larger during *in situ* generation in the fractured systems as a result of fewer snap-off sites in the fracture compared to the Berea sandstone used for bubble pre-generation. The resulting foam texture and the relationship of curvature with foam viscosity determined the flow resistance of the system. Similar snap-offs in idealized fractures at the transition from narrow to large aperture was reported [40], where the flow resistance increased with greater gas fractional flow and larger aperture. Similarly, flow in rough-walled fractures was previously characterized [39, 41], and may be favourable for mobility in fracture networks of varying aperture [42].

4. Experimental procedures

In this work, experiments providing insight to polymer gel behaviour during and after placement were performed using cylindrical outcrop core plugs with a 1 mm longitudinal fracture and aged to varying wetting states. *In situ* imaging by CT, MRI and PET was used to quantify and explain local saturation behaviour during polymer gel placement and chase-floods. Foam was investigated using a fractured marble tile model encased in Plexiglas that enabled us to visualize and describe foam flow in fractures (the marble itself is impermeable) at different gas fractions.

4.1. Establishing stable wettability preferences by dynamic ageing

Stable, predictable and uniformly distributed wettability preference is essential during core analysis to achieve reliable results [43–45]. The simplest wettability preference to achieve is the *strongly water-wet* condition, where the contact angle between oil and water on a smooth surface is between 0° and 30° [46]. All clean outcrop rocks are strongly water-wet before exposure to crude oil, and a strongly water-wet wettability preference may be achieved and maintained using mineral oils [47]. However, this wettability preference does not reflect the preference of most reservoirs [48], and it is therefore needed to change the wettability of outcrop cores to better reflect reservoir conditions. Because core plugs extracted from the subsurface are exposed to drilling muds and large changes in pressure and temperature conditions during extraction, wettability alteration is also needed for reservoir cores [49]. Based on a decade of wettability alteration studies in chalk [50–54], a dynamic wettability alteration method [55] is outlined below

1. Cylindrical core plugs are drilled from outcrop rock blocks and cut to length. The core plugs are thereafter washed in tap water and dried at 60°C for no less than a week. The core plugs are thereafter saturated by brine, and porosity, and permeability measured.

2. The crude oil is prepared for ageing by being heated to 90°C and thereafter injected through a chalk core at a constant injection rate to remove impurities. Before use, the chalk core filter is flooded with crude oil to low water saturation and aged by flushing crude oil through the core at 1 cm^3/h for 96 h, reversing the flow direction midways. The crude oil used for ageing the filter core plug is not re-used in the wettability alteration study. Due to its aged state, it was assumed that the adsorption of active wettability alteration components on the filter was significantly reduced. After filtration, the crude oil is stored in closed containers at 90°C with minimal interference and without air exposure until used to age the cores.

3. The fully water saturated core plugs are oilflooded to irreducible water saturation by crude oil injection at high differential pressures (2 bar/cm) at 90°C. When S_{wi} is reached, the injection rate is reduced to an ageing flow rate of 3 cm^3/h or 1.5 cm^3/h, for 2″ and 1.5″ diameter cores, respectively. Crude oil is continuously injected throughout the entire ageing process, and the direction of flow reversed midway. The ageing time is determined by the crude oil/rock/brine system and the desired wettability preference. After ageing, the crude oil is miscibly displaced from the core with 5PV of decaline (decahydronaptha-lene) followed by 5PV mineral oil (e.g. decane), all at 90°C.

4. Wettability is measured using the Amott-Harvey method: spontaneous and forced imbibition of water, followed by spontaneous and forced imbibition of the preferred mineral oil: using mineral oil to represent the oil phase ensures that the wettability of the core plugs is not further altered for the duration of experiments.

5. Experiments to investigate enhanced oil recovery (EOR) potential are commonly started at the irreducible water saturation, S_{wi}.

4.2. Imaging techniques applied in porous media

Several imaging techniques are currently applied to study flow in porous media, and most techniques originate from medical imaging. Here, we briefly review three imaging techniques used to study mobility control for EOR in fractured core plug systems.

4.2.1. Positron emission tomography (PET)

PET is based on positron-emitting radionuclides where a positron is emitted from the nucleus accompanied by an electron to balance atomic charge. Radioactivity is a spontaneous nuclear phenomenon insensitive to temperature and pressure [56]. The positron loses kinetic energy by interactions with the surroundings, and at near-zero momentum the positron combines with an electron and annihilates. The use of PET to study flow in porous media was recently reviewed and compared with CT [57]. Spatial fluid saturation is calculated based on the registered activity of the labelled phase, which in this work is water using the fluorine radioisotope [18]F.

4.2.2. X-ray computed tomography (CT)

CT measures the X-ray attenuation through gradual loss in flux intensity through the medium, and produces a time-averaged density distribution image of the rock [58, 59]. CT imaging relies on sufficient density contrasts which may often be fulfilled in low-porosity media. Because attenuation depends on both the electron density and the effective atomic number, the CT number will vary with the energy of the rays. Spatial fluid saturation is derived with sufficient fluid density difference.

4.2.3. Magnetic resonance imaging (MRI)

MRI provides high spatial resolution imaging and fast data acquisition necessary to study flow in porous media. When replacing hydrogen in the aqueous phase (H_2O) with deuterium (D_2O), the magnetic signal in the water phase is removed and one explicit fluid phase (oil) is imaged in an oil-water system. MRI has successfully been used to characterize flow behaviour and production mechanisms in fractured chalk and their dependency on wettability, injection rate, fracture aperture and configurations [56, 60].

Figure 1 shows the different views applied during *in situ* imaging of cylindrical core plugs in this study. The sagittal view was often used to capture the flow dynamics inside the open fracture—which was vertically aligned in all experiments.
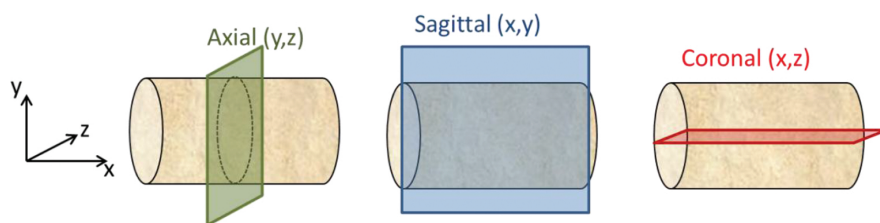
Figure 1. Schematic representation of the different views applied during *in situ* imaging of a core plug.

5. Recent advances in laboratory evaluation of polymer gel and foam for EOR

5.1. *In situ* imaging of polymer gel transport in fractured core plugs

Complementary *in situ* imaging techniques have been used to investigate different aspects of polymer gel treatments described in the following sections. For most experiments, artificially fractured core plugs with open, longitudinal fractures have been used and the matrix has been saturated by two immiscible phases: oil and water, to mimic the environment in an oil reservoir. The polymer gel used for all experiments was 0.5% HPAM (~5 million daltons molecular weight) cross-linked by 0.04% (417 ppm) Cr(III)-acetate and aged at 41°C for 24 h (five times the gelation time). After ageing, the gel was cooled to ambient temperature of ~23°C.

5.1.1. Gel shrinkage from spontaneous imbibition

Gel placement in fractured reservoirs and its behaviour during chasefloods have been widely studied [4, 15, 61], but gel interaction with the porous rock in which the fractures are embedded has been less discussed. The exchange of fluids between the gel and adjacent porous rock may be substantial, even without a viscous pressure gradient across the system, if spontaneous capillary imbibition of water occurs [23]. Spontaneous imbibition impact leakoff during gel placement and gel stability after placement, and the loss of water from the gel is influenced by relative permeability, capillary pressure and the wettability of the porous medium. A severe reduction in gel volume (up to 99%) was documented due to spontaneous imbibition into porous media from adjacent, non-flowing bulk gel [23], suggesting that gel treatments lose efficiency over time where a potential for spontaneous imbibition exists, because gel-treated fractures may be opened to flow. Polymer gel is often used to reduce water cut and is therefore placed in a well or zone of the reservoir that is watered-out, where spontaneous imbibition is reduced. During EOR operations, however, the local fluid saturations may change considerably, i.e. if an oil bank is generated, and spontaneous imbibition may again have impact on gel mobility control.

5.1.2. Leakoff dependency on wettability

In a strongly water-wet rock, a positive capillary force exists to attract water from the gel into the rock matrix. In an oil-wet rock, however, water will be repelled and must overcome a capillary threshold pressure to invade the pores. These two wettability conditions were directly compared using complementary imaging techniques during mature gel injection into open fractures. Cylindrical core plugs with longitudinal fractures of 1 mm aperture were used, and gel was injected with a constant volumetric injection rate into the fracture at ambient conditions.

In strongly water-wet, low-permeable chalk rock samples, where a strong positive capillary pressure exists, residual oil saturations were reached during gel placement due to water leakoff [25]. The chalk core was placed in a Bruker 4.7T MRI, and a spin-echo based sequence was used to produce images during D_2O-gel injection. MRI settings must be tuned for each experiments, and depend strongly on the core material used, the fluid saturation and type of experimental setup (e.g. if a core holder or epoxy layers were used as confinement vessel). Finding the right settings for each experiment requires expert knowledge of the imaging apparatus and is not the focus of this chapter. Readers are referred to [62]. **Figure 2** shows MRI images of water leakoff during gel placement in a low-permeable, strongly water-wet chalk core (permeability, K <10 mD, porosity, φ = 45%, d = 4.96 cm, L = 7.6 cm). The rock matrices adjacent to the fracture were initially fully saturated with mineral oil (*n*-decane) and appear light grey in the images. Bedding planes in the rock sample may be observed as darker features that are constant in the images. A strong positive capillary pressure exists due to the small pore sizes of this rock [63]. Water leaves the gel during leakoff and reduces the oil saturation in the rock matrix adjacent to the fracture first (darker grey regions due to loss of magnetic signal from the oil).
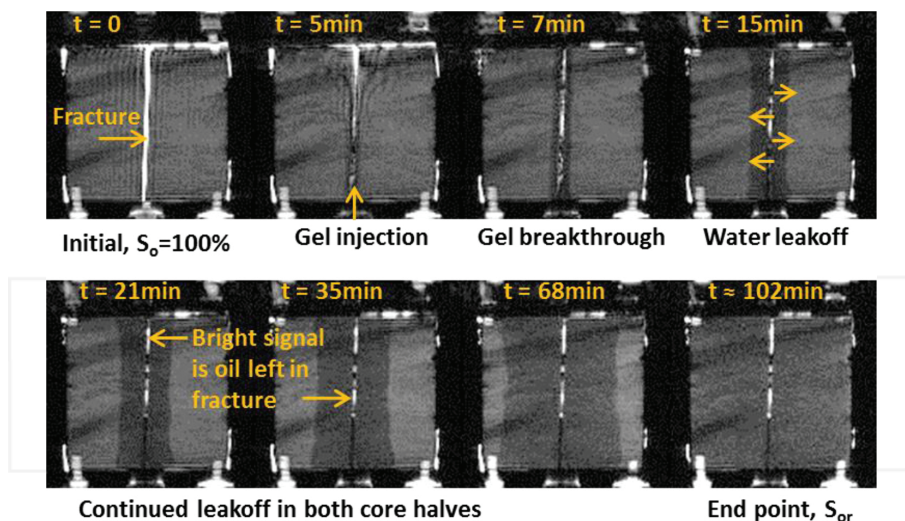
Figure 2. Coronal slices through a cylindrical, fractured core plug placed in an MRI during gel placement. As D_2O-gel (no signal) progress through the fracture, conventional material balance experiments suggest that the oil in the fracture is displaced; however, the MRI images shown here suggest that some oil remains in the fracture even after significant gel flooding.

The water leakoff from the gel in the fracture to the oil-saturated matrix was symmetric around the fracture and occurred by combined spontaneous and forced imbibition from the differential pressure generated. This combined displacement resulted in residual oil saturation in the matrix after gel placement, corresponding to 64% OOIP oil recovery during gel injection for the chalk core used. Although significant oil was produced in experiments at core plug scale, gel placement will not in itself contribute significantly to oil production at field scale because of the small fracture volume (1–2%) relative to matrix volume in most reservoirs. Hence, chasefloods are important to recover additional oil after a gel placement. The concept of gel placement is, however, important to study because it greatly affects the success of chaseflood oil recovery.

In oil-wet and low permeable rocks, a threshold pressure must be overcome to achieve water leakoff. Local water leakoff during mature gel placement in a fractured, oil-wet carbonate core plug (K = 11.7 mD, φ = 17.6%, d = 3.8 cm, L = 10.1 cm) was investigated by CT [64]. The CT was a Picker PQ-6000 with 120 kV_P tube voltage. Scans were produced with 4 s scanning time, and the slice thickness was 2 mm. Using a low injection rate of 6 cm^3/h during gel injection reduced the differential pressure and no leakoff was observed. Gel progressed through the fracture without losing water and increasing its concentration—thus, rock saturation remained constant at the irreducible water saturation (**Figure 3**, top and middle). In fully water saturated rock, where capillary forces are not present, the differential pressure limit to achieve leakoff corresponds to the pressure needed to extrude gel through the fracture [3]. Improved sweep efficiency was observed during the subsequent chaseflood when the injected water displaced oil from the rock matrix, predominantly in the inlet part of the core (see **Figure 3**).
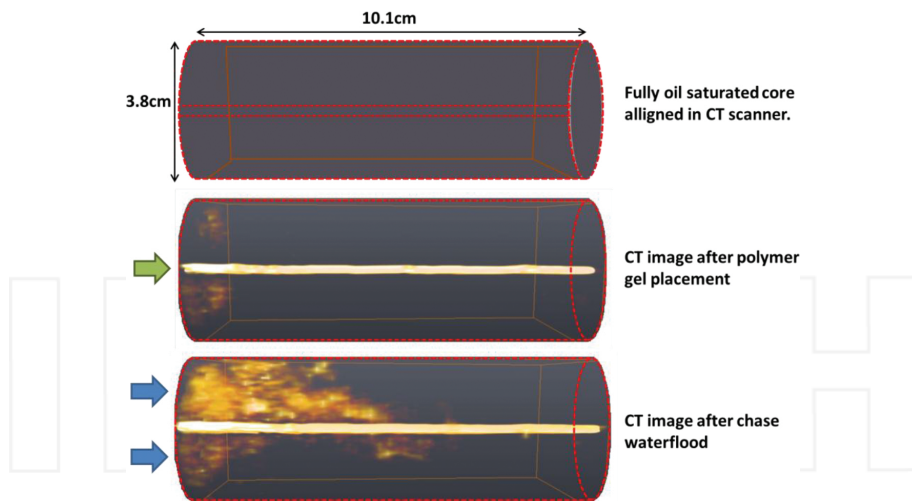
Figure 3. CT images of a fractured core plug. Top: the core is aligned in the CT at S_{wi}. Middle: CT image taken after gel placement. A strong signal from the gel is seen throughout the fracture. Matrix saturation changes were not observed during gel placement. Bottom: Chase waterflooding. A dispersed chase water front was clearly distinguishable by CT.

### 5.2. Visualization of EOR chaseflood behaviour

During gel placement in initially oil-filled fractured systems, it is assumed that the oil residing in the fracture is produced at gel breakthrough [25]. This assumption was based on the high differential pressure observed during chasefloods, comparable to conventional experiments using 100% water saturated cores.

5.2.1. Oil trapped in gel

Upon careful inspection of **Figure 2**, it is possible to observe oil remaining in the fracture (bright sections) during gel flooding, and also after significant gel throughput. A clear rupture pressure during water chaseflooding suggests that the oil did not impact the blocking capacity of the gel. By employing the MRI further to image the chaseflood (**Figure 4**), we determined that the water flow paths were narrow and presumably through wormholes in the dehydrated gel, and that the oil remaining in the fracture was trapped within the gel structure (light grey areas in **Figure 4**). **Figure 4** shows the water flow paths through the gel in the fracture (bright white). A thresholded image (**Figure 4B**) shows the wormhole flow pattern in more detail.

Wormhole size is known to change with injection rate due to the gel elasticity. Although the gel pressure resistance is stable at low injection rates (below 600 cm^3/h, corresponding to a maximum injection flux of 1100–1600 cm/h when all flow of water is through the fracture), the gel may erode in the vicinity of wormholes at higher injection rates over time (significant water throughput). In experiments where the purpose is to measure wormhole size, it is therefore advisable to use high flow rates within relatively short time intervals. Without imaging, the

average wormhole size can be calculated indirectly by measuring the injection rate and average pressure drop across the core plug. With *in situ* imaging, such as applying PET, the wormhole size may be measured directly, and the wormhole dynamics with changes in injection rate directly observed. Wormholes within a gel-filled fracture were observed and quantified using PET, as shown in **Figure 5**. PET/CT sequences were acquired on a CT 80 W Nanoscan PC imager, featuring spatial resolutions of 800 and 30 μm of the respective PET- and CT-detector systems. The core used was of Edwards limestone material [65] and was fully saturated by brine with a composition equal to the gel solvent. The PET signal was not corrected for attenuation in the analysis because the low CT tube energy (70 kV_P) did not penetrate the core to produce spatial core plug density (needed for attenuation correction). The CT was thus only used for core plug positioning. In **Figure 5**, radioactively labelled water (^{18}FDG) was injected into the gel-filled fracture with a constant injection rate of 60 cm^3/h. When the pressure drop had stabilized across the core (at 1.6 kPa/cm for this injection rate), the wormhole flow pattern, visualized by PET, remained unchanged and covered 22.3% of the fracture volume. Dehydrated gel (no signal) covered the remaining fracture volume. *In situ* imaging by PET showed locally large variations in the wormhole width, from very narrow (almost invisible on images) in some sections of the fracture to spanning large parts of the fracture height in other sections.
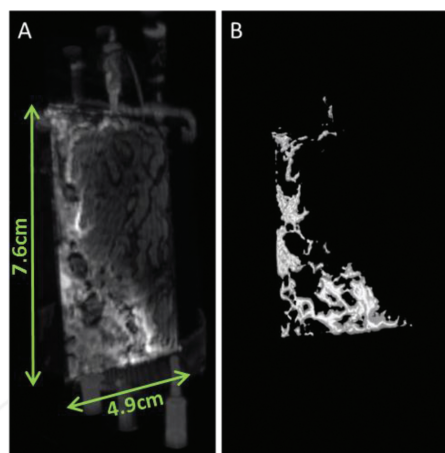

Figure 4. (A) Three-dimensional image of the core plug during water chaseflooding. All remaining signal is in the fracture. Grey areas represent *n*-decane, whereas white signal represent the intruding water phase. (B) With signal thresholding the water phase may be separated from the oil to exhibit the wormhole pattern.

Waterflooding after polymer gel placement may be efficient, and even if the gel has ruptured it provides significantly reduced fracture conductivity compared to open fractures. *In situ* imaging of core floods (**Figure 3**) have, however, shown that displacement fronts may be dispersed during water chasefloods. Enhanced oil recovery may be achieved by stabilizing the displacement front, e.g. using foam [64]. The gel treatment may also be strengthened after placement by injecting a water phase with lower salinity relative to the water in the gel [66]. Both injection pressures and matrix production rates during chasefloods increased with

reduced salinity compared with chasefloods where the salinity was matched with the gel [25], presumably due to swelling of the polymer gel network. The improvement of the polymer gel treatment was reversible, and gel blocking efficiency immediately decreased during chasefloods with matched salinity. This shows that is possible to control the success of a chaseflood by influencing the gel properties. Combining polymer gel placement in fractures with low-salinity chasefloods is therefore a promising approach in iEOR. The new findings from PET imaging (**Figure 5**) may be helpful in explaining the mechanism for improved conformance control during low-salinity chase waterfloods and shed light on wormhole morphology when injected water salinity is varied.
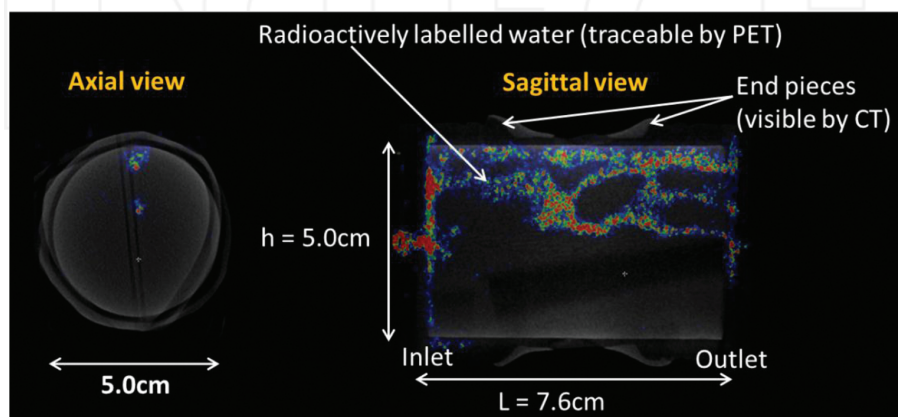
Figure 5. Positron emission tomography (PET) during radioactive chase waterflooding of a fractured core where gel has been placed in the fracture. The wormholes in the fracture are clearly seen and their development may be tracked as a function of flow rate and time. The colour pixels represent different spatial concentrations of brine in the fracture: the red signal corresponds to a high spatial concentration of radioactively labelled water, compared to e.g. blue colour (low spatial concentration). CT is applied to correctly position the PET signal in the core space.

5.3. Fractured tile model to investigate 2D foam flow in fractured systems

An experimental setup was built to visualize flow and to study mobility control by foam generation in fracture networks. A white marble tile was fractured using a ball-peen hammer and then carefully reassembled within a frame to create a fracture network with rough, calcite fracture surfaces. The (effective) porosity was assumed to be zero in the marble matrix blocks, and flow occurred through the fracture network only. The fracture network was characterized by injecting brine and gas separately into the model. Pure nitrogen (N_2) gas injection provided a baseline to which foam injection could be compared. **Figure 6** shows the marble tile model filled with red-dyed brine.

Aqueous surfactant solution (1 wt% alpha olefin sulfonate (AOS) surfactant in 5 wt% NaCl brine) and N_2-gas were co-injected into the fracture network at ambient conditions to form foam, using a range of gas fractions, to investigate the impact of the gas fraction on sweep

efficiency. The fracture network was initially filled with aqueous solution, and the total flow rate for the co-injections was 60 cm^3/h.


Figure 6. A square marble tile was fractured and reassembled within an aluminium frame sandwiched between two Plexiglas plates. The fracture network consisted mainly of narrow fractures with 12 large fractures. The vugular open fractures were larger bodies of open space varying between 0.4 and 2.2 cm aperture. These cavities were used to observe the advancing foam front during co-injection. In this figure, the marble tile model is filled with red-dyed brine to emphasize the fracture network.

5.3.1. Sweep efficiency

Areal sweep efficiency with changes in gas fraction was evaluated using the fracture network: a high-resolution camera was used to capture images at short time intervals throughput foam co-injection. From the images, total sweep was evaluated and it was possible to map flow patterns and calculate dynamic sweep efficiency as function of foam volume injected. Images could capture drainage of liquid from each fracture element, including vugs and narrow fractures. **Figure 7** compares total areal sweep efficiency for three N$_2$-gas fractions during foam co-injection: fg = 0.60, fg = 0.80 and fg = 0.90.

Figure 7 shows the development in sweep efficiency within the fracture network during co-injection with three different gas fractions. The sweep efficiency is compared at three time steps: after three fracture elements are filled; after five fracture elements and after seven fracture elements are filled. Only foam in the larger vugs could be visualized directly, but foam was also generated in, and flowed through, the smaller apertures. In general, we see that the sweep efficiency and spread of foam was higher with the increase of gas fractional flow. At higher gas fractions, breakthrough of gas was delayed, but in all cases delayed compared with pure gas injection. This demonstrated that foam reduced gas mobility and was formed within the fracture network itself.
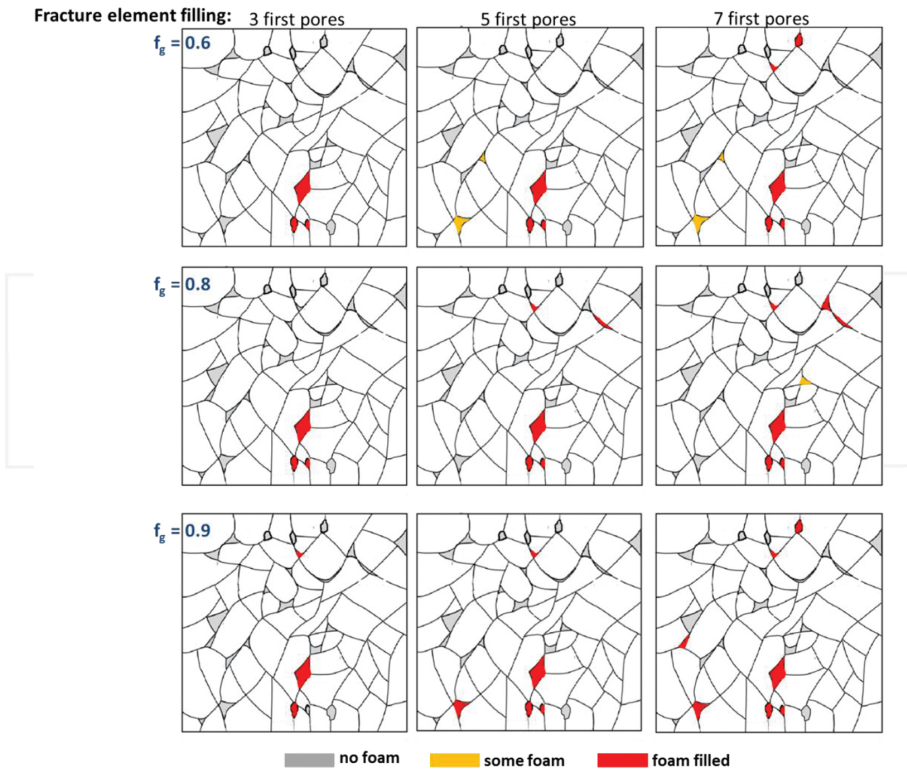
Figure 7. Foam propagation through a fractured marble tile system. Foam filling of the first three, five and seven frac-ture elements are shown for gas fractions of 60% (top), 80% (middle) and 90% (bottom), respectively. Co-injection was performed bottom to top in the images.

Unlike the foam bubble shape in a porous medium, where bubble shape is governed by pore configurations [35, 67], the bubbles in fractures are deformed according to interfacial tension, and the gas-liquid interfacial curvature varies according to gas fractional flow [41]. Foam coalescence in a porous medium is controlled by the 'limiting-capillary-pressure' [68] at moderate to high gas fractional flow. The limiting capillary pressure is determined by the pore size, surfactant formulation, local fluid saturation and the interstitial velocity. The capillary pressure in a fracture is much lower (generally set to zero in most simulations—although strictly not correct) at a given aqueous-phase saturation in comparison to permeable matrix. Capillary suction coalescence of foam lamellae appeared to become significant when the local aqueous phase saturation became very low. With increased gas fraction, the gas bubbles increased in size, on average. Large gas bubbles separated by thin lamellae occupied the majority of the fracture volume, especially at 0.95 gas fraction. This effect may be attributed to thinning of lamella at high gas fractional flow [69], resulting in foam coalescence and merging of smaller bubbles. Fewer and coarser bubbles related to the highest gas fraction are likely caused by thinning of lamellae (a larger fraction of the liquid is located in the Plateau border),

followed by film rupture due to higher capillary-suction pressure compared to lower gas fractional flow. The observations are consistent with earlier results, where larger bubbles were observed with increased gas fractional flow in a fracture network [39, 70].

5.4. Combined polymer gel and foam chasefloods for iEOR

Using a low-field 8 MHz MRI (Oxford Instruments Maran DRX), we experimentally investigated an iEOR approach where the first step was polymer gel placement to reduce fracture conductivity and the second step was CO_2-foam injection to improve sweep efficiency compared to water chasefloods [64]. The experiments were performed at ambient conditions, thus the CO_2 was not miscible with the oil (*n*-decane). Pre-generated foam was injected into the core after gel placement, using a gas fraction of 0.8 and a surfactant solution containing 1 wt% AOS surfactant. The development in oil saturation during all experimental steps was compared to oil recovery during foam injection without mobility control, using magnetic resonance imaging. Two fractured carbonate core plugs were used ($K \approx 30$ mD, φ = 23–24%, d = 3.8 cm, L = 5.8 cm), with a measured Amott-Harvey wettability index after dynamic ageing of I_{AH} = −0.2, which represents weakly oil-wet conditions. Waterfloods were not efficient due to the oil-wet conditions and only recovered 10–20% of the oil in place. *In situ* imaging showed that oil was primarily displaced from the inlet end of the core plugs, where water was injected directly into the matrix through specially designed end pieces [64]. Oil was displaced into the fracture, and no further oil recovery from the core matrix was detected after water breakthrough. Polymer gel placement was performed at 100 cm^3/h and yielded 20% oil recovery that was caused by the large fracture volume compared to the core pore volume at high injection pressure and low matrix threshold pressure due the weak oil-wet conditions. Chaseflooding by immiscible CO_2-foam was performed to mitigate fluid dispersion around the displacement front. **Figure 8** shows the *in situ* development of the oil saturation and displacement fronts during foam flooding in the twin cores, with and without polymer gel conformance control present in the fracture. Oil production was prevailing in the near-fracture area by direct foam injection (**Figure 8A**). Haugen et al. [71] showed, using CT imaging of oil-wet core plug systems, that oil was viscously displaced by surfactant solution, forced into the matrix by the increased pressure gradient provided by the foam. In **Figure 8B**, polymer gel was placed in the fracture prior to CO_2-foam flooding, and both foam constituents (gas and surfactant solution) entered the matrix during the foam flood. Immiscible foam injection after conformance control by polymer gel provided 28% OOIP (original oil in place) additional oil recovery during 12.7 PV foam injected. In comparison, recovery factors of 14% OOIP (**Figure 8A**) to 20% OOIP were obtained during injection of more than 30 PV foam in comparable core plugs. Improved sweep efficiency was visually observed by MRI during foam chasefloods (**Figure 8**); in which more stable displacement fronts and less tendency to viscous fingering were observed when compared to e.g. chase waterflooding. The combination of two established EOR methods to improve conformance in both the fracture and matrix has important implications for future work on the development of efficient integrated EOR schemes.
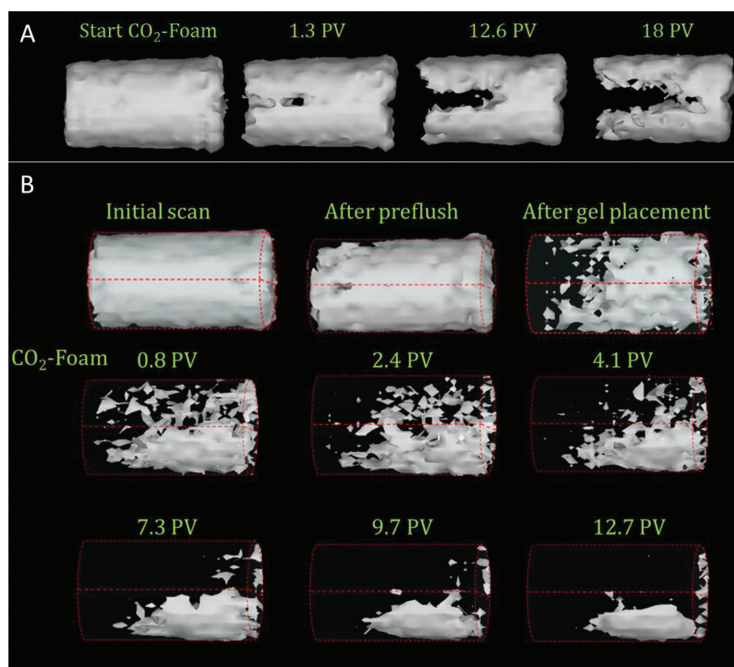
Figure 8. Development in *in situ* oil saturation (light grey areas) during foam flooding of fractured, oil-wet carbonate core plugs: (A) directly after waterflooding and (B) with polymer gel present in the fracture. Injections were performed left to right.

6. Conclusions

In situ imaging provides new insight and corroborates results from core analysis applying material balance or gravimetrical measurements, and several different imaging techniques may be used to closely investigate local changes in saturation, fluid flow and oil recovery mechanisms during EOR experiments. Using *in situ* imaging techniques in this work, we found that:

- Water leakoff during polymer gel propagation through a fractured, oil-saturated core plug could be captured using magnetic resonance imaging (MRI). Water leakoff was symmetric around the fracture and occurred by combined spontaneous and forced imbibition from the differential pressure generated by the gel injection.

- Residual oil within the gel structure was observed with MRI after gel injection into a fractured, oil-saturated core plug. The remaining oil did not impact the flow paths during water chasefloods, and it is likely that only a thin oil layer partly coated some region of the gel.

- Water flow paths known as wormholes were observed during chase waterfloods applying positron emission tomography (PET). We found large local variations in the wormhole shape and width that have not previously been observed during waterfloods. PET is able to catch rapid changes in fluid saturation during dynamic floods and may thus give valuable information about changes in wormhole morphology as a function of flow rate and pressure.

- *In situ* imaging by CT and MRI were used to investigate the shape of displacement fronts during chasefloods when polymer gel had been placed in a fracture. Imaging showed a dispersed displacement front during waterflooding of an oil-wet core plug. CO_2-foam injection stabilized the displacement front and improved sweep efficiency.

Advanced medical imaging is not always required or available, and important insight may be gained from relatively simple experimental setups, such as the study foam generation in fractures where Plexiglas models provide the visualization needed. We found that foam was generated in a fracture model during co-injection of surfactant and N_2-gas. A higher fractional flow of gas increased the sweep efficiency and spread of foam in vugs and fractures.

The crux of core plug scale experiments is proper design and planning of the experimental schedule using suitable equipment and imaging tools. When the core plug system is positioned within the imaging apparatus it cannot be moved. Hence, Testing the experimental setup without imaging, using simple material balance, is a good idea.

Author details

Bergit Brattekås[1] and Martin A. Fernø[2*]

*Address all correspondence to: martin.ferno@uib.no

1 National Improved Oil Recovery Centre, University of Stavanger, Stavanger, Norway

2 Department of Physics and Technology, University of Bergen, Bergen, Norway

References

[1] Liang, J.-T., R.L. Lee, and R.S. Seright, Gel Placement in Production Wells. SPE Production and Facilities, 1993. 8(November): p. 276–284.

[2] Seright, R.S., Gel Placement in Fractured Systems. SPE Production & Facilities, 1995. 10(4): p. 241–248.

[3] Seright, R.S., Gel Propagation Through Fractures. SPE Production & Facilities, 2001. 16(4): p. 225–231.

[4]   Seright, R.S., Washout of Cr(III)-Acetate-HPAM Gels from Fractures, in International Symposium on Oilfield Chemistry. 2003, Society of Petroleum Engineers: Houston, TX.

[5]   Ganguly, S., et al., The Effect of Fluid Leakoff on Gel Placement and Gel Stability in Fractures. SPE Journal, 2002. 7(03): p. 309–315.

[6]   McCool, C.S., X. Li, and G.P. Wilhite, Flow of a Polyacrylamide/Chromium Acetate System in a Long Conduit. SPE Journal, 2009. 14(01): p. 54–66.

[7]   Brattekås, B., et al., Washout of Cr(III)-Acetate-HPAM Gels From Fractures: Effect of Gel State During Placement. SPE Production & Operations, 2015. 30(02): p. 99–109.

[8]   Seright, R.S., An Alternative View of Filter-Cake Formation in Fractures Inspired by Cr(III)-Acetate-HPAM Gel Extrusion. SPE Production & Facilities, 2003. 18(1): p. 65–72.

[9]   Seright, R.S., et al., Improved Methods for Water Shutoff, in Final Technical Progress Report (US DOE Report No. DOE/PC/91008-14), US DOE Contract No. DE-AC22-94PC91008, BDM-Oklahoma Subcontract No. G4S660330. 1998. p. 21–54.

[10] Seright, R.S., R.H. Lane, and R.D. Sydansk, A Strategy for Attacking Excess Water Production. SPE Production and Facilities, 2003. 18(03): p. 158–169.

[11] Sydansk, R.D., A Newly Developed Chromium(III) Gel Technology. SPE Reservoir Engineering, 1990. 5(03): p. 346–352.

[12] Sydansk, R.D. and G.P. Southwell, More Than 12 Years Experience With a Successful Conformance-Control Polymer-Gel Technology. SPE Production & Operations, 2000. 15(4): p. 270–278.

[13] Portwood, J.T. Lessons Learned from Over 300 Producing Well Water Shut-Off Gel Treatments. in SPE Mid-Continent Operations Symposium. 1999. Oklahoma City, OK, USA.

[14] Portwood, J.T., The Kansas Arbuckle Formation: Performance Evaluation and Lessons Learned From More Than 200 Polymer-Gel Water-Shutoff Treatments, in SPE Productions and Operations Symposium. 2005: Oklahoma City, OK, USA.

[15] Willhite, G.P. and R.E. Pancake, Controlling Water Production Using Gelled Polymer Systems. SPE Reservoir Evaluation & Engineering, 2008. 11(3): p. 454–465.

[16] Wilton, R. and K. Asghari, Improving Gel Performance in Fractures: Chromium Pre-Flush and Overload. Journal of Canadian Petroleum Technology, 2007. 46(02).

[17] Zou, B., et al., Precipitation of Chromium Acetate Solutions. SPE Journal, 2000. 5(03): p. 324–330.

[18] Vossoughi, S., Profile Modification Using In Situ Gelation Technology—A Review. Journal of Petroleum Science and Engineering, 2000. 26(1–4): p. 199–209.

[19] Romero-Zeron, L.B., F.M. Hum, and A. Kantzas, Characterization of Crosslinked Gel Kinetics and Gel Strength by Use of NMR. SPE Reservoir Evaluation and Engineering, 2008. 11(03): p. 439–453.

[20] Dawe, R.A. and Y. Zhang, Mechanistic Study of the Selective Action of Oil and Water Penetrating into a Gel AMplced in a Porous Medium. Journal of Petroleum Science and Engineering, 1994. 12(2): p. 113–125.

[21] Al-Sharji, H.H., et al., Pore-Scale Study of the Flow of Oil and Water through Polymer Gels, in SPE Annual Technical Conference and Exhibition. 1999, Society of Petroleum Engineers: Houston, TX.

[22] Krishnan, P., et al., Dehydration and Permeability of Gels Used in In-Situ Permeability Modification Treatments, in SPE/DOE Improved Oil Recovery Symposium. 2000, Society of Petroleum Engineers: Tulsa, OK.

[23] Brattekås, B., et al., Gel Dehydration by Spontaneous Imbibition of Brine from Aged Polymer Gel. SPE Journal, 2014. 19(01): p. 122–134.

[24] Bai, B.J., et al., Preformed Particle Gel for Conformance Control: Factors Affecting its Properties and Applications. SPE Reservoir Evaluation & Engineering, 2007. 10(4): p. 415–422.

[25] Brattekås, B., A. Graue, and R.S. Seright, Low Salinity Chase Waterfloods Improve Performance of Cr(III)-Acetate HPAM Gel in Fractured Cores, in SPE International Symposium on Oilfield Chemistry. 2015, Society of Petroleum Engineers: The Wood-lands, TX, USA.

[26] Horkay, F., I. Tasaki, and P.J. Basser, Osmotic Swelling of Polyacrylate Hydrogels in Physiological Salt Solutions. Biomacromolecules, 2000. 1: p. 84–90.

[27] Zuta, J. and I. Fjelde, Transport of CO_2-Foaming Agents During CO_2-Foam Processes in Fractured Chalk Rock. SPE Reservoir Evaluation & Engineering, 2010. 13(4): p. 710–719.

[28] Chen, C.-Y. and R.N. Horne, Two-phase Flow in Rough-walled Fractures: Experiments and a Flow Structure Model. Water Resources Research, 2006. 42(3): p. W03430.

[29] Fourar, M., et al., Two-phase Flow in Smooth and Rough Fractures: Measurement and Correlation by Porous-medium and Pipe Flow Models. Water Resources Research, 1993. 29(11): p. 3699–3708.

[30] Pruess, K. and Y.W. Tsang, On Two-phase Relative Permeability and Capillary Pressure of Rough-walled Rock Fractures. Water Resources Research, 1990. 26(9): p. 1915–1926.

[31] Auradou, H., et al., Enhancement of Velocity Contrasts by Shear-thinning Solutions Flowing in a Rough Fracture. Journal of Non-Newtonian Fluid Mechanics, 2008. 153(1): p. 53–61.

[32] Di Federico, V., Estimates of Equivalent Aperture for Non-Newtonian Flow in a Rough-walled Fracture. International Journal of Rock Mechanics and Mining Sciences, 1997. 34(7): p. 1133–1137.

[33] Rossen, W.R., Foams in Enhanced Oil Recovery, in Foams: Theory, Measurements, and Applications, R.K. Prud'homme and S.A. Khan, Editors. 1995, Marcel Dekker, Inc.: New York.

[34] Bertin, H.J., et al., Foam Flow in Heterogeneous Porous Media: Effect of Cross Flow. SPE Journal, 1999. 4(2).

[35] Ransohoff, T.C. and C.J. Radke, Mechanisms of Foam Generation in Glass-Bead Packs. SPE Reservoir Engineering, 1988. 3(2): p. 573–585.

[36] Tanzil, D., G.J. Hirasaki, and C.A. Miller, Mobility of Foam in Heterogeneous Media: Flow Parallel and Perpendicular to Stratification. SPE Journal, 2002. 7(2): p. 203–212.

[37] Falls, A.H., et al., Development of a Mechanistic Foam Simulator: The Population Balance and Generation by Snap-Off. SPE Reservoir Engineering, 1988. 3(03): p. 884–892.

[38] Rossen, W.R., Foam Generation at Layer Boundaries in Porous Media. SPE Journal, 1999. 4(4): p. 409–412.

[39] Kovscek, A.R., et al., Foam Flow Through a Transparent Rough-walled Fracture. Journal of Petroleum Science and Engineering, 1995. 17: p. 75–86.

[40] Buchgraber, M., L.M. Castanier, and A.R. Kovscek, Microvisual Investigation of Foam Flow in Ideal Fractures: Role of Fracture Aperture and Surface Roughness, in SPE Annual Technical Conference and Exhibition. 2012, Society of Petroleum Engineers: San Antonio, Texas, USA.

[41] Pancharoen, M., M.A. Ferno, and A.R. Kovscek, Modeling Foam Displacement in Fractures. Journal of Petroleum Science and Engineering, 2012. 100: p. 50–58.

[42] Yan, W., C.A. Miller, and G.J. Hirasaki, Foam Sweep in Fractures for Enhanced Oil Recovery. Colloids and Surfaces A: Physicochem. Eng. Aspects 2006(283–284): p. 348–359.

[43] Spinler, E.A., B.A. Baldwin, and A. Graue, Experimental Artifacts Caused by Wettability Variations in Chalk. Journal of Petroleum Science and Engineering, 2002. 33(1–3): p. 49–59.

[44] Graue, A., et al., Alteration of Wettability and Wettability Heterogeneity. Journal of Petroleum Science and Engineering, 2002. 33(1–3): p. 3–17.

[45] Aspenes, E., A. Graue, and J. Ramsdal, In Situ Wettability Distribution and Wetting Stability in Outcrop Chalk Aged in Crude Oil. Journal of Petroleum Science and Engineering, 2003. 39(3–4): p. 337–350.

[46] Anderson, W., Wettability Literature Survey—Part 2: Wettability Measurement. SPE Journal of Petroleum Technology, 1986. 38(11): p. 1246–1262.

[47] Graue, A., E. Tonheim, and B.A. Baldwin. Control and Alteration of Wettability in Low-Permeability Chalk. in Proc.: 3rd International Symposium on Evaluation of Reservoir Wettability and Its Effect on Oil Recovery. 1995. Laramie, WY, USA.

[48] Morrow, N.R., Wettability and Its Effect on Oil Recovery. Journal of Petroleum Technology, 1990. 42(12): p. 1476-1484.

[49] Anderson, W.G., Wettability Literature Survey—Part 1: Rock/Oil/Brine Interactions and the Effects of Core Handling on Wettability. SPE Journal of Petroleum Technology, 1986. 38(10): p. 1125–1144.

[50] Graue, A., B.G. Viksund, and B.A. Baldwin. Reproduce Wettability Alteration of Low-Permeable Outcrop Chalk. in SPE/DOE Improved Oil Recovery Symposium. 1998. Tulsa, Oklahoma: Society of Petroleum Engineers.

[51] Graue, A., et al., Systematic Wettability Alteration by Aging Sandstone and Carbonate Rock in Crude Oil. Journal of Petroleum Science and Engineering, 1999. 24(2–4): p. 85–97.

[52] Graue, A., et al. Impacts of Wettability on Capillary Pressure and Relative Permeability. in International Symposium of the Society of Core Analysts. 1999. Golden, CO, USA.

[53] Graue, A., B.G. Viksund, and B.A. Baldwin, Reproducible Wettability Alteration of Low-Permeable Outcrop Chalk. SPE Reservoir Evaluation & Engineering, 1999. 2(2): p. 134–140.

[54] Graue, A., et al., Wettability Effects on Oil-Recovery Mechanisms in Fractured Reservoirs. SPE Reservoir Evaluation & Engineering, 1999. 4(6).

[55] Fernø, M.A., et al., Dynamic Laboratory Wettability Alteration. Energy & Fuels, 2010. 24(7): p. 3950–3958.

[56] Ersland, G., et al., Complementary Imaging of Oil Recovery Mechanisms in Fractured Reservoirs. Chemical Engineering Journal, 2010. 158: p. 32–38.

[57] Fernø, M.A., et al., Combined Positron Emission Tomography and Computed Tomography to Visualize and Quantify Fluid Flow in Sedimentary Rocks. Water Resources Research, 2015.

[58] Heindel, T.J., A Review of X-Ray Flow Visualization With Applications to Multiphase Flows. Journal of Fluid Engineering-Transactions of ASME, 2011. 133(7).

[59] Blunt, M.J., et al., Pore-scale Imaging and Modelling. Advances in Water Resources, 2013. 51(0): p. 197–216.

[60] Aspenes, E., et al., Wetting Phase Bridges Establish Capillary Continuity Across Open Fractures and Increase Oil Recovery in Mixed-Wet Fractured Chalk. Transport in Porous Media, 2008. 74(1): p. 35–47.

[61] Seright, R.S., R.H. Lane, and R.D. Sydansk, A Strategy for Attacking Excess Water Production, in SPE Permian Basin Oil and Gas Recovery Conference. 2001, Copyright 2001, Society of Petroleum Engineers Inc.: Midland, Texas.

[62] Oleg, P., G. Ersland, and A. Graue, T2-distribution Mapping Profiles with Phase-encode MRI. Journal of Magnetic Resonance, 2011. 209(1): p. 39–46.

[63] Johannesen, E.B., NMR Characterization of Wettability and How it Impacts Oil Recovery in Chalk, in Department of Physics and Technology. 2008, University of Bergen: Bergen. p. 71.

[64] Brattekås, B., et al., Fracture Mobility Control by Polymer Gel- Integrated EOR in Fractured, Oil-Wet Carbonate Rocks, in EAGE Annual Conference & Exhibition incorporating SPE Europec. 2013: London, UK.

[65] Tie, H., Oil Recovery by Spontaneous Imbibition and Viscous Displacement from Mixed-wet Carbonates, in Department of Chemical and Petroleum Engineering. 2006, The University of Wyoming: Laramie, Wyoming. p. 238.

[66] Tu, T.N. and B. Wisup, Investigating the Effect of Polymer Gels Swelling Phenomenon under Reservoir Conditions on Polymer Conformance Control Process, in International Petroleum Technology Conference. 2011, International Petroleum Technology Conference: Bangkok, Thailand.

[67] Mast, R.F., Microscopic Behavior of Foam in Porous Media, in Fall Meeting of the Society of Petroleum Engineers of AIME. 1972, Society of Petroleum Engineers: San Antonio, Texas.

[68] Khatib, Z.I., G.J. Hirasaki, and A.H. Falls, Effects of Capillary Pressure on Coalescence and Phase Mobilities in Foams Flowing Through Porous Media. SPE Reservoir Engineering, 1988. 3(3): p. 919–926.

[69] Gauteplass, J., et al., Pore-level Foam Generation and Flow for Mobility Control in Fractured Systems. Colloids and Surfaces A: Physicochemical and Engineering Aspects, 2015. 468(0): p. 184–192.

[70] Fernø, M.A., et al., Experimental Study of Foam Generation, Sweep Efficiency and Flow in a Fracture Network, in SPE Annual Technical Conference and Exhibition. 2014, Society of Petroleum Engineers: Amsterdam, The Netherlands.

[71] Haugen, Å., et al., Miscible and Immiscible Foam Injection for Mobility Control and EOR in Fractured Oil-wet Carbonate Rocks. Transport in Porous Media, 2014(104): p. 109–131.